NASA TN D-1823

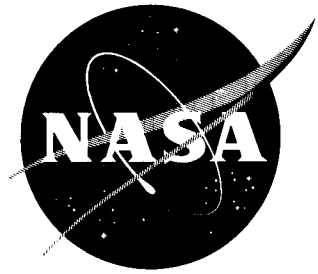

TECHNICAL NOTE

D-1823

AERODYNAMIC CHARACTERISTICS IN PITCH AT A MACH NUMBER OF 2.01 OF SEVERAL WING-BODY COMBINATIONS WITH WEDGE-SHAPED BODIES LOCATED ABOVE AND BELOW A 54.5° SWEPT DELTA WING

By Odell A. Morris

Langley Research Center
Langley Station, Hampton, Va.

NATIONAL AERONAUTICS AND SPACE ADMINISTRATION
WASHINGTON

June 1963

NATIONAL AERONAUTICS AND SPACE ADMINISTRATION

TECHNICAL NOTE D-1823

AERODYNAMIC CHARACTERISTICS IN PITCH AT A MACH NUMBER OF 2.01 OF SEVERAL WING-BODY COMBINATIONS WITH WEDGE-SHAPED BODIES LOCATED ABOVE AND BELOW A 54.5° SWEPT DELTA WING

By Odell A. Morris

SUMMARY

An investigation has been conducted at a Mach number of 2.01 to determine the aerodynamic characteristics in pitch of several model configurations with wedge-shaped bodies located above and below a 54.5° swept delta wing. The investigation included tests on bodies of wedge-shaped planform with variations in body wedge angle, body height, and body length. Measurement of the lift, drag, and pitching-moment coefficients for the various wing-body combinations were made through an angle-of-attack range of about -5° to 10°.

The results of the investigation indicated that large changes in lift-drag ratio occurred as a result of the wing-body interference effects produced by the presence of the combined wedge-shaped bodies located above and below the delta wing. However, for all of the wedge-shaped bodies tested, addition of the body to the wing tended to reduce the maximum lift-drag ratio from that of the basic wing-body combination. The interference effects of the two bodies in combination with the wing produced a favorable positive pitching-moment increment. For the range of body combinations tested, the magnitude of the lift-drag ratios is dependent to a great extent on the variation in body volume.

INTRODUCTION

In an effort to find supersonic configurations that provide improved lift-drag ratios, a number of studies have been made in recent years on various ways of shaping or arranging wing-body combinations to produce favorable interference effects. One phase of these studies has been concerned with the effects of locating a body above or below a wing and shaping the body so that favorable lifting pressures are produced by the body on the wing. (See refs. 1 to 4.) The investigations of references 1 to 3 were theoretical studies and indicated that possible improvements in lift-drag ratio may be obtained by utilizing thin bodies shaped to produce favorable interference effects on the wing, but no

correlation of the results was made with experimental values. The experimental pressure investigations of reference 4 provided results for a series of wedge-shaped bodies located below a triangular wing and these results indicated that location of the basic wedge body shapes under the wing did not produce improvements in the maximum lift-drag ratios at a Mach number of 3.11. The investigation was limited, however, to body shapes located only on the lower wing surface.

Thus, the present investigation has been conducted in the Langley 4- by 4-foot supersonic pressure tunnel at a Mach number of 2.01 to determine the aerodynamic characteristics of several wing-body configurations with wedge-shaped bodies located above and below a delta wing. The investigation included tests on bodies of wedge-shaped planform with variation in body wedge angle, body height, and body length through an angle-of-attack range of about -5° to 10° at a Reynolds number per foot of 2.41×10^{6}. The lift, drag, and pitching-moment characteristics of the configurations, together with some oil-flow photographs, are presented with a limited analysis.

SYMBOLS

All force and moment coefficients are referred to the wind-axis system. The pitching-moment coefficients are referenced to the wing center line at a station 9.90 inches from the leading edge of the wing root chord.

b	wing span
$\bar{c}$	wing mean aerodynamic chord
C_D	drag coefficient, Drag/qS
C_L	lift coefficient, Lift/qS
C_m	pitching-moment coefficient, Pitching moment/$qS\bar{c}$
h	height of body
L/D	lift-drag ratio
q	free-stream dynamic pressure
S	total wing area
V	volume of test body
α	angle of attack, measured from the wing center-line chord to the tunnel free-stream flow angle, deg
δ	wedge semiangle of body planform

MODELS AND APPARATUS

The principal dimensions of the basic wing body model are shown in figure 1(a). The 54.5° swept delta wing was constructed of steel and had symmetrical double-wedge wing sections (maximum thickness at 0.50 wing chord), which were 2 percent thick. Other dimensional characteristics include the following:

Wing span, in.	26.15
Mean aerodynamic chord, in.	12.21
Wing area, sq ft	1.66
Aspect ratio	2.84

The full-span wing was sting mounted in the tunnel. A six-component balance was attached directly to one side of the wing and was housed in a minimum size wedge-shaped body designated as body A. Thus, body A, which was a modified 6° wedge-shaped body, was mounted on one surface of the wing as shown in figure 1(a) for

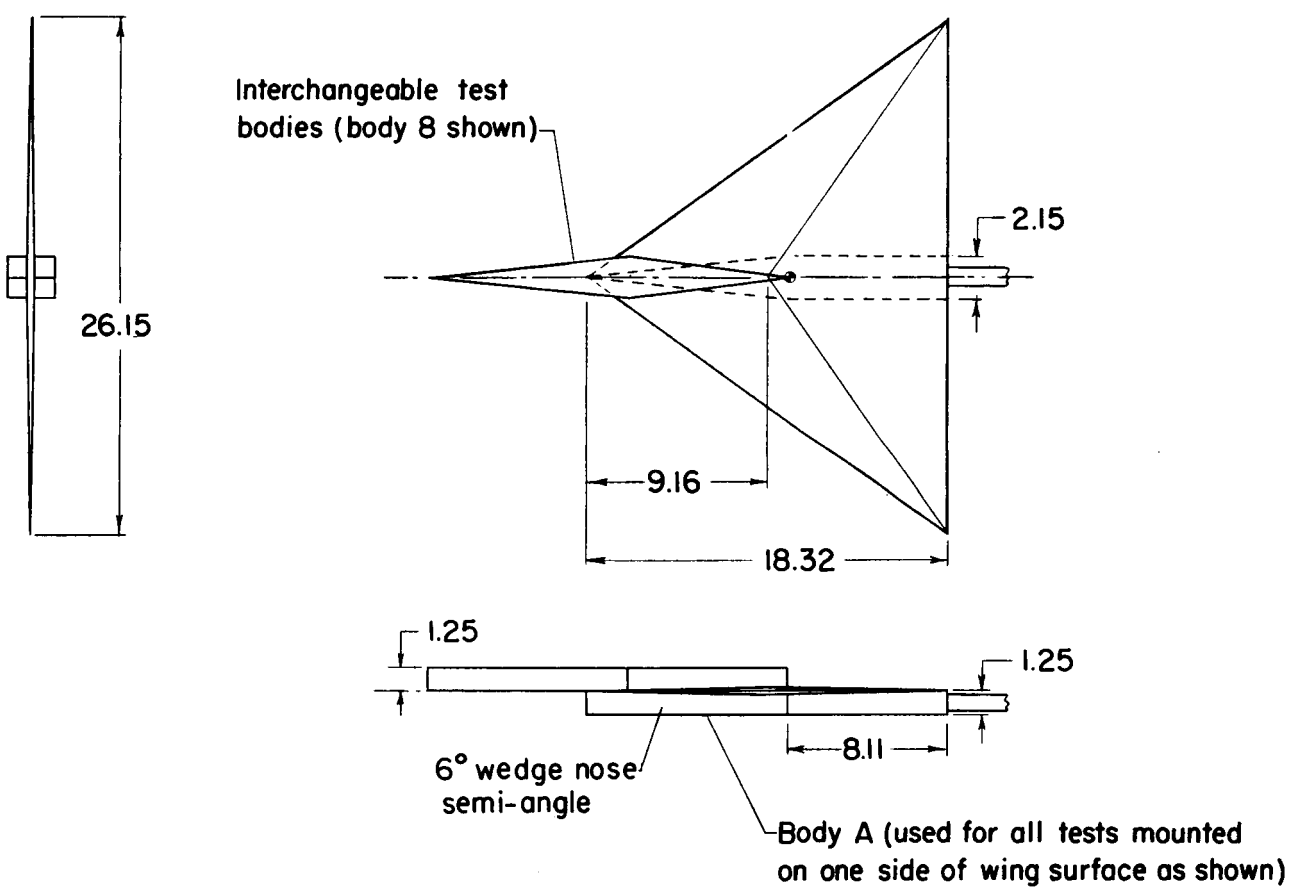

(a) Wing-body combination.

Figure 1.- Details of models. (All dimensions in inches unless otherwise noted.)

all tests made during the investigation. The various test bodies were mounted on the opposite surface of the wing and were considered to be above or below the wing, depending on the particular body shape tested. The body shapes tested as below-wing bodies are shown in figure 1(b) and are designated as bodies 1 to 7. The test bodies considered as above-wing bodies are shown in figure 1(c) and are designated as bodies 8 to 11. All test bodies were simple flat-sided and flat-bottom wedge shapes with rectangular body cross sections and were constructed of wood.

TESTS, CORRECTIONS, AND ACCURACY

The investigation was conducted in the Langley 4- by 4-foot supersonic pressure tunnel at the following test conditions:

Mach number	2.01
Stagnation temperature, ^{o}F	110
Stagnation pressure, lb/sq in.	10
Reynolds number per foot	2.41×10^{6}

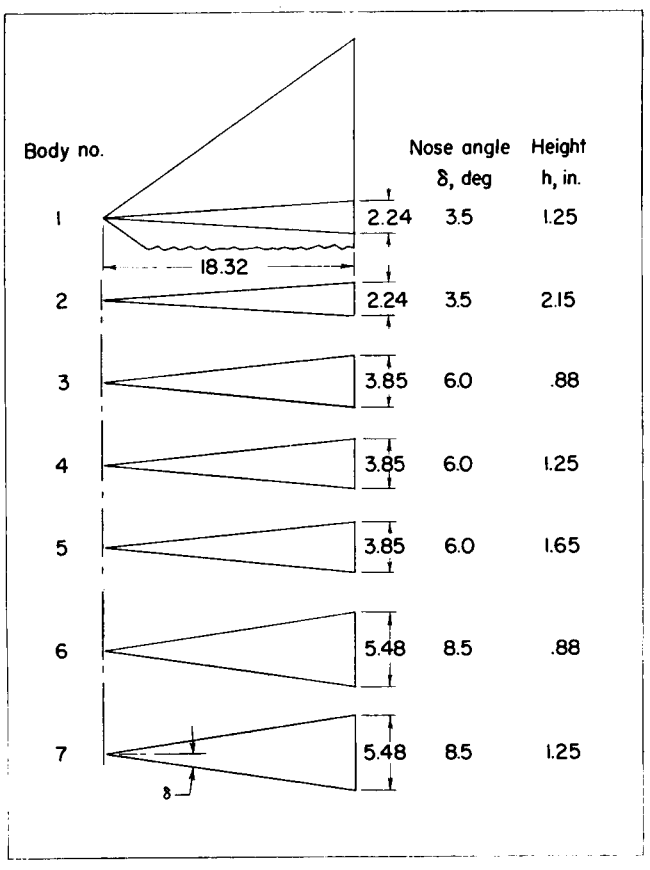

(b) Various body shapes tested below wing.

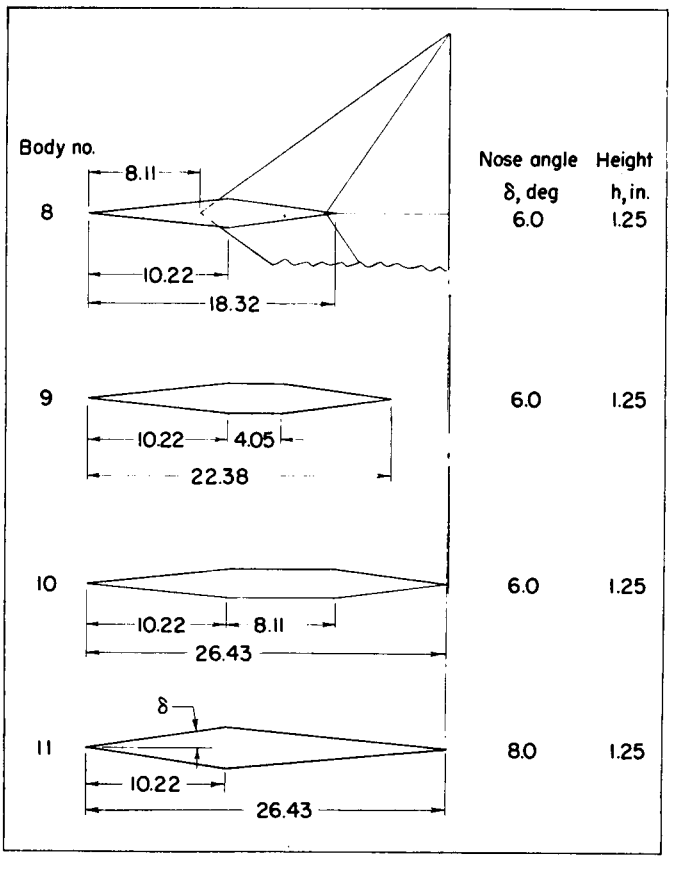

(c) Various body shapes tested above wing.

Figure 1.- Concluded.

The models were sting mounted, and tests of the complete models in pitch covered an angle-of-attack range of about -5° to 10°. The forces and moments were measured by means of an internal six-component strain-gage balance. The angles of attack were corrected for deflection of the balance and sting attributable to aerodynamic load. The base pressures of the blunt-base bodies were measured and the drag forces were adjusted to correspond to a condition at which base pressure would be equal to free-stream static pressure. All tests were made with transition fixed on the wing and on the bodies. The transition strips consisted of 1/8-inch-wide strips of No. 80 carborundum grains on both sides of the wing and around the nose of the bodies approximately 1/4 inch back from the leading edges of the various components. In the course of the tests, oil-flow photographs were made of several of the configurations to indicate the flow conditions on the model surfaces. These photographs are shown in figure 2.

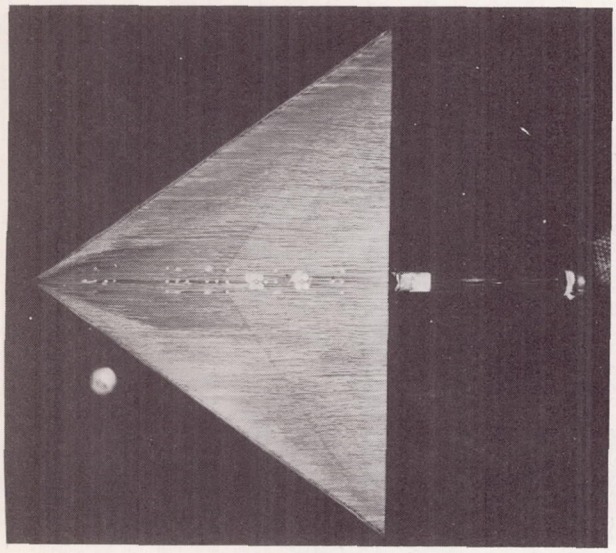

$\alpha = .39°$

(a) Wing lower surface.

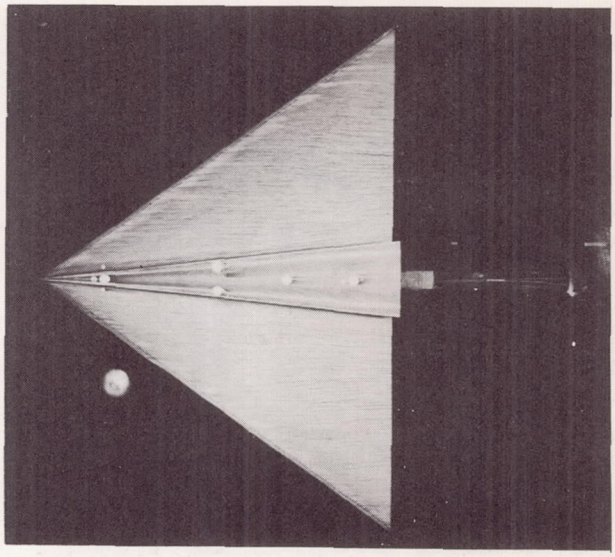

$\alpha = .35°$

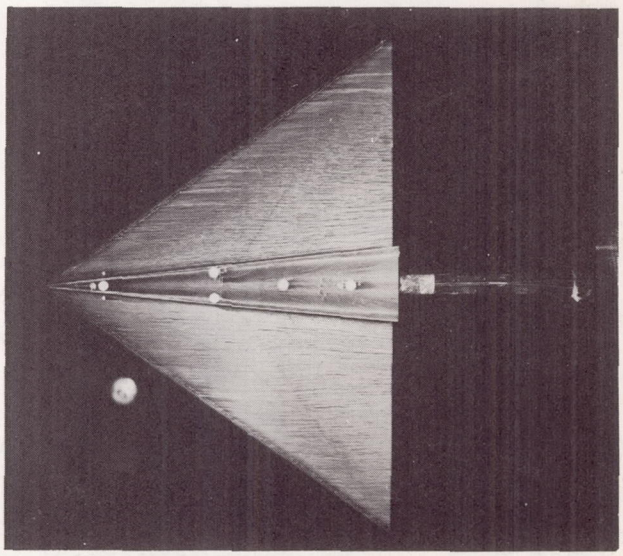

$\alpha = 4.13°$

(b) Body 4 below wing.

L-63-3109

Figure 2.- Oil-flow photographs of several test configurations.

The estimated accuracy of the measured quantities is as follows:

C_L	±0.0010
C_D	±0.0008
C_m	±0.0010
α, deg	±0.1

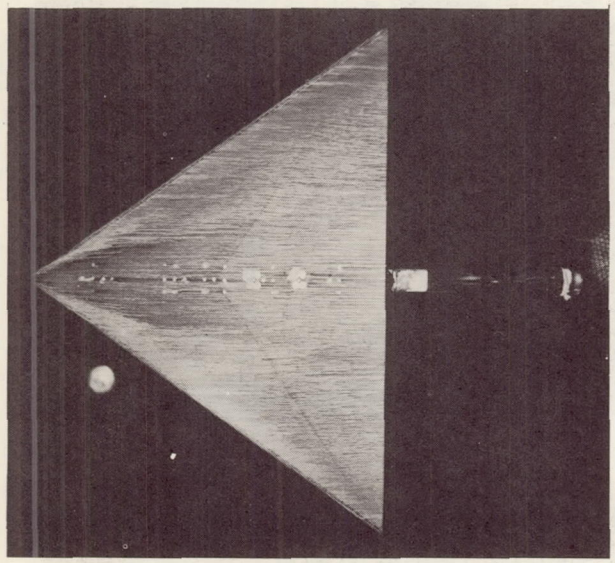

$\alpha = .39°$

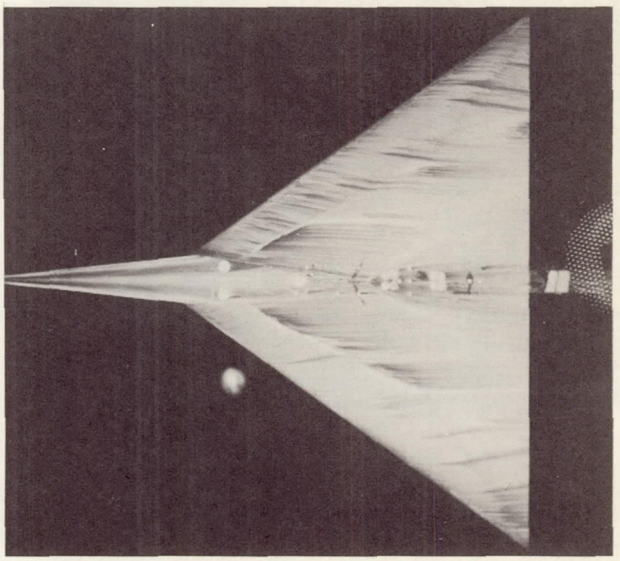

$\alpha = .41°$

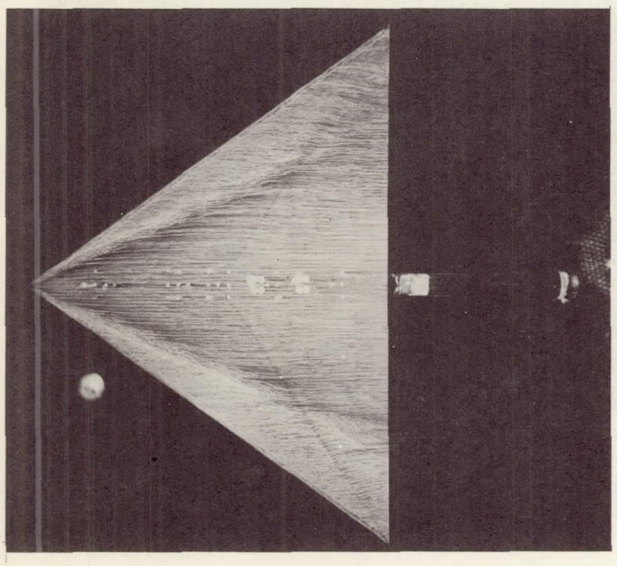

$\alpha = 4.12°$

(c) Wing upper surface.

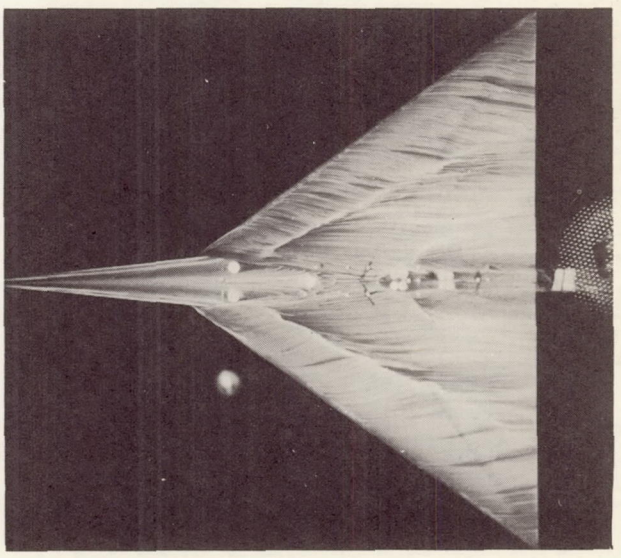

$\alpha = 4.20°$

(d) Body 8 above wing.

Figure 2.- Continued. L-63-3110

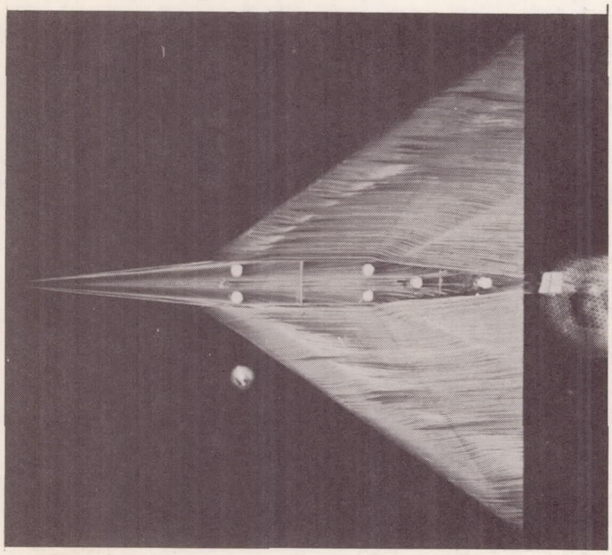

$\alpha = .44°$

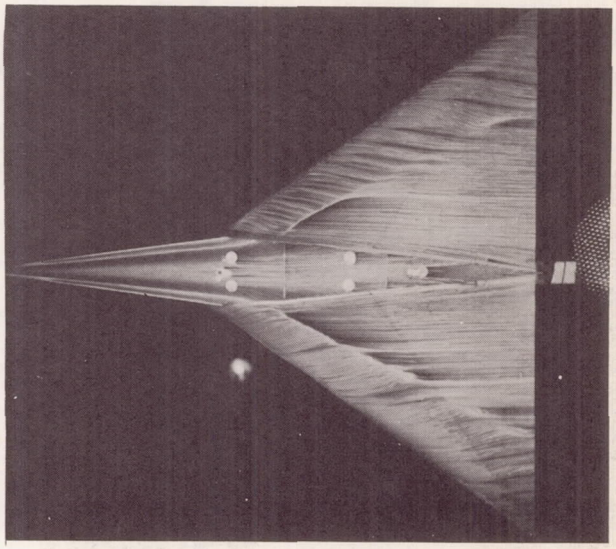

$\alpha = .50°$

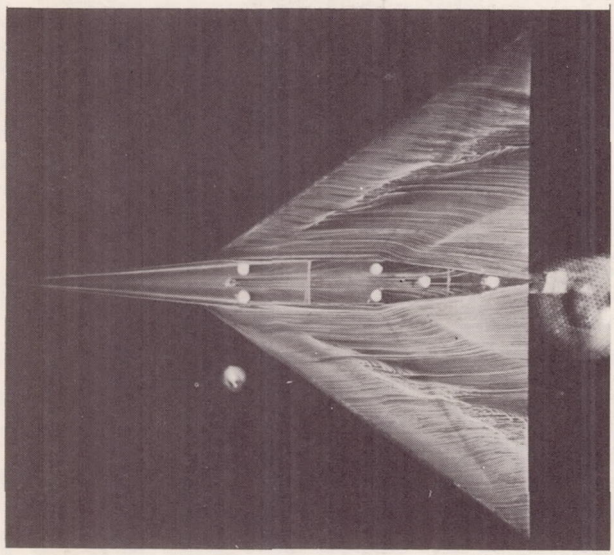

$\alpha = 4.19°$

(e) Body 10 above wing.

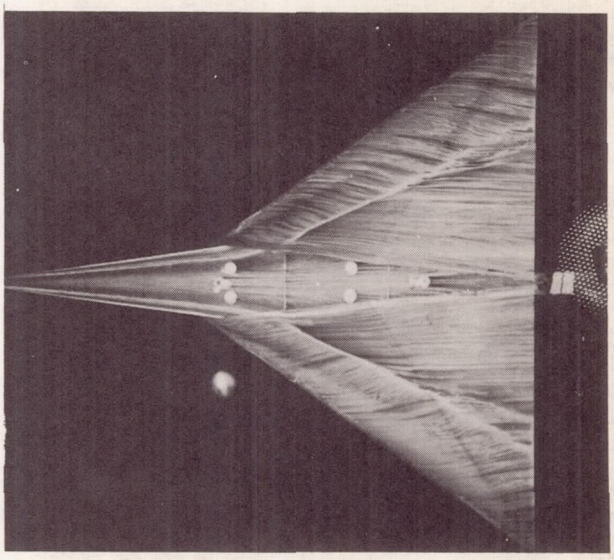

$\alpha = 4.28°$

(f) Body 11 above wing.

Figure 2.- Concluded. L-63-3111

RESULTS AND DISCUSSION

The aerodynamic characteristics in pitch for the basic wing-body combination (body A only) are presented in figure 3. The data of figures 4, 5, and 6 present the data for the under-wing wedge-shaped bodies 1 to 8. For these figures, it should be noted that body A is located on the top surface of the wing; therefore, the aerodynamic characteristics of the wing-body combination shown include the effects of this basic body. However, the incremental differences measured between the coefficients for the various test bodies will give an indication of the wing-body interference effects due to the variation in body shape. As was pointed out in reference 4, wedge-shaped bodies with large base areas and corresponding large base drag would have little practical application unless the base areas could be utilized to contain jet exits. Therefore, all drag data presented herein have been corrected for base pressures as noted previously.

The data of figure 4 show that increasing the body wedge angle from 3.5° to 8.5° for a constant body height produced positive increases in the lift coefficients, which were fairly constant through the angle-of-attack range. However, the drag coefficients also increased with increase in wedge angle in such a way that the maximum L/D values were reduced.

Increasing the body wedge height from 0.88 to 1.25 inches for a constant wedge angle of 6° (fig. 5) also tends to show a decrease in maximum L/D values, although the differences were small. It might be pointed out, however, that the variation in body wedge height increased the body volume by about 85 percent as compared with an increase in body volume of about 48 percent for the variation in body wedge angle.

A comparison of the aerodynamic characteristics for three wedge-body shapes having varying wedge angle and body heights, but with equal volume $\left(\frac{V^{2/3}}{S} = 0.057\right)$ showed no significant changes in any of the measured components. (See fig. 6.) Thus, these results, together with the data of figures 4 and 5 indicate that for the range of wedge-shaped bodies tested, the magnitude of the L/D ratios are dependent to a great extent on the variation in body volume.

The data of figures 7 and 8 present the aerodynamic characteristics for several wing-body combinations with the wedge-shaped test bodies located on the top surface of the wing. For these configurations, the basic body A is located below the wing, which provides a combined top and bottom wedge body arrangement where both bodies should be providing some favorable interference effects on the wing.

Figure 7 shows a comparison of the data for the three wing-body combinations with test bodies having different body lengths and slightly different body shapes. The effect of the wedge-shaped bodies on the top surface of the wing was similar to the effect produced by the bodies on the bottom wing surface inasmuch as increasing the body volume tended to decrease the maximum L/D values. Figure 8 shows the aerodynamic characteristics for a wing-body combination with a

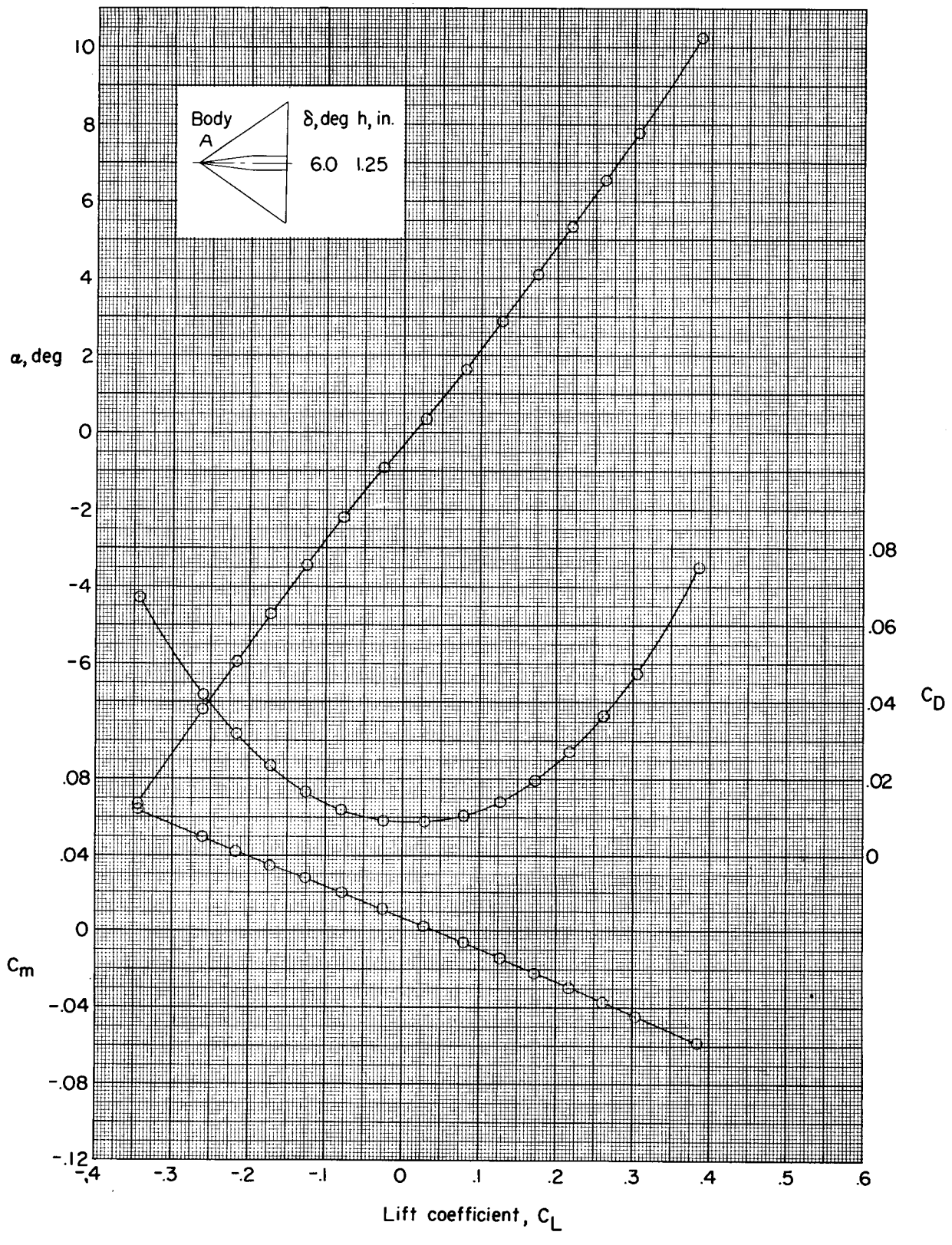

(a) Variation of α, C_m, and C_D with C_L.

Figure 3.- Aerodynamic characteristics in pitch of the basic wing-body combination only. Body A located below wing.

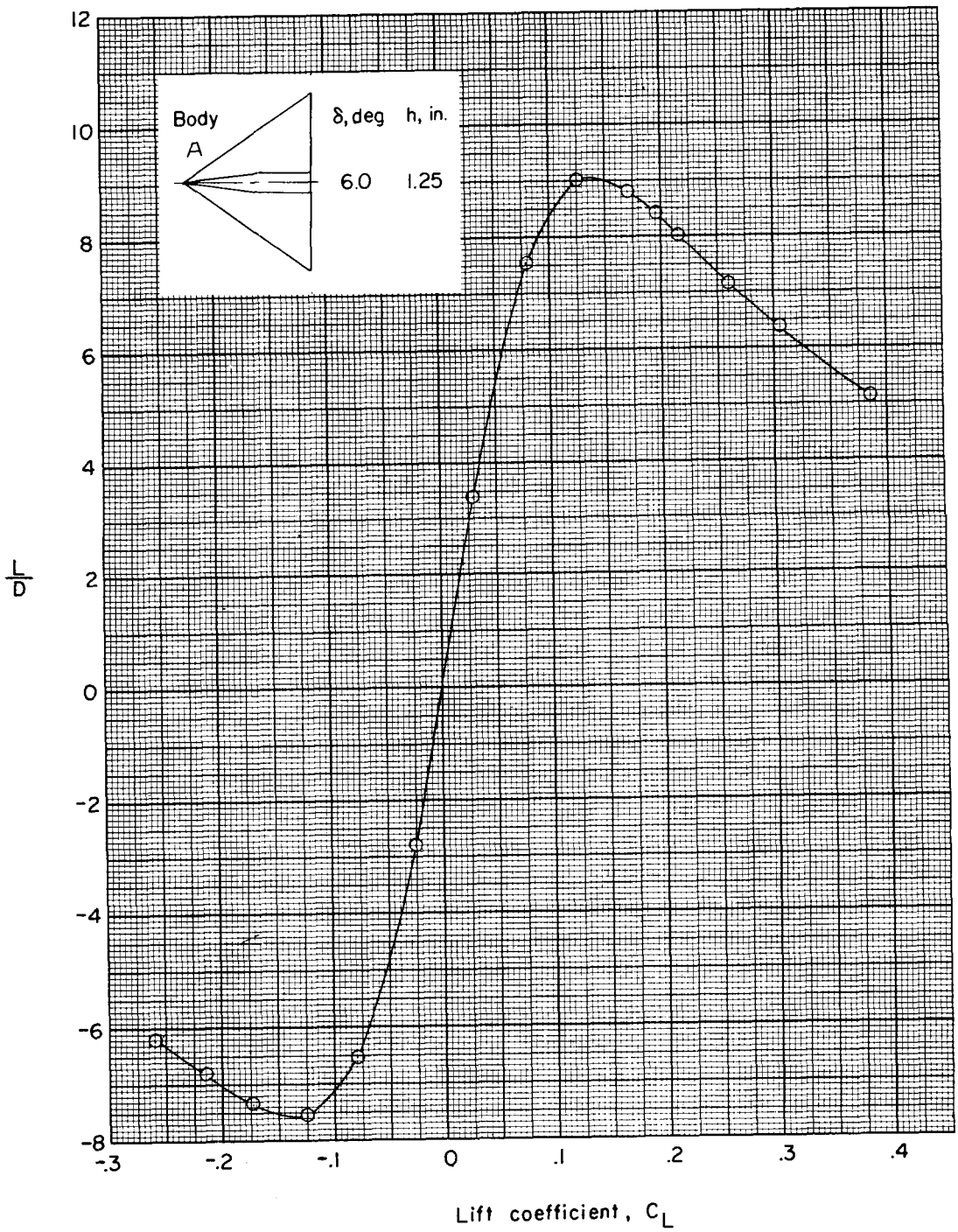

(b) Variation of L/D with C_L.

Figure 3.- Concluded.

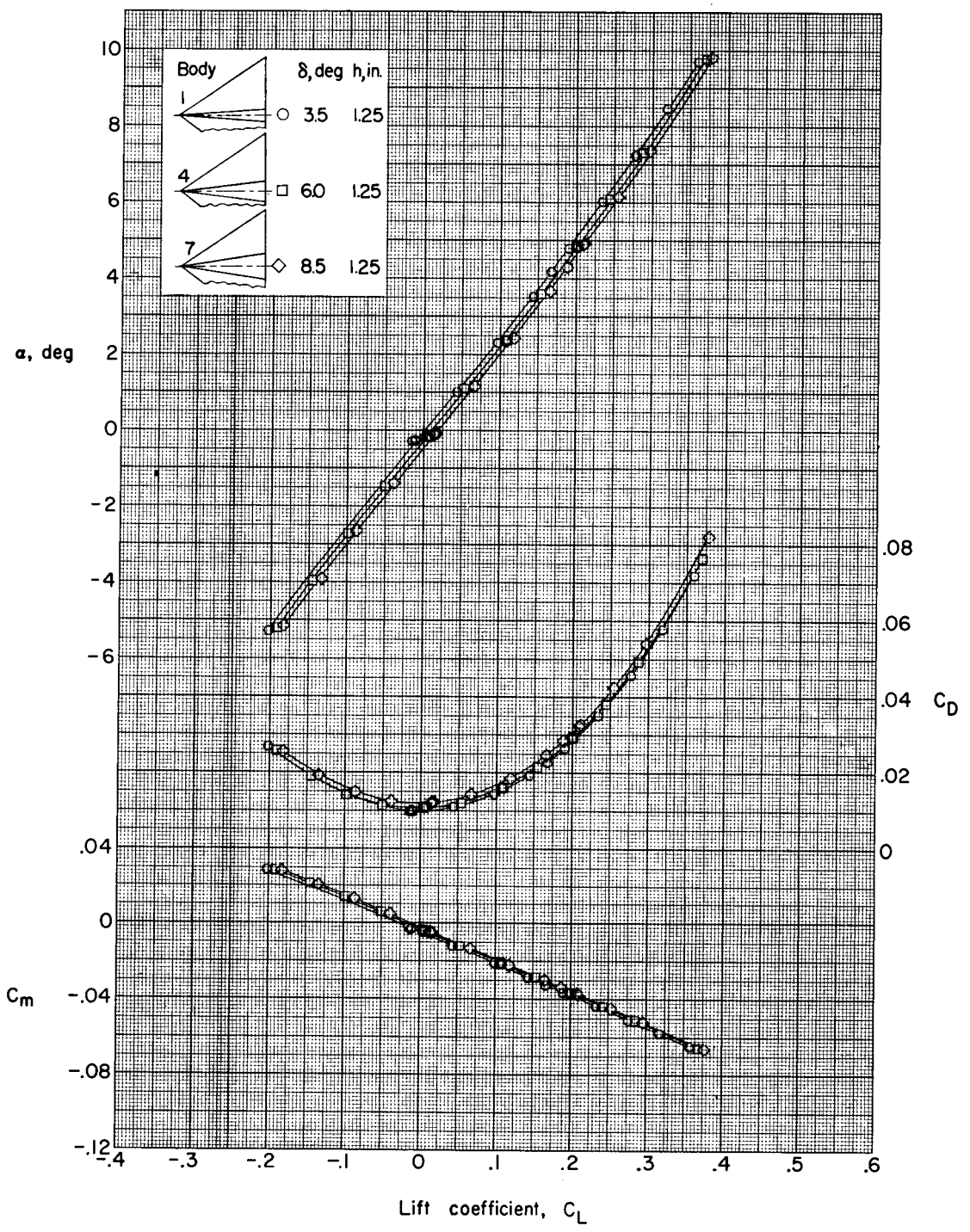

(a) Variation of α, C_m, and C_D with C_L.

Figure 4.- Effect of change in body wedge angle on the aerodynamic characteristics in pitch for the wing-body combination. Body A located above wing.

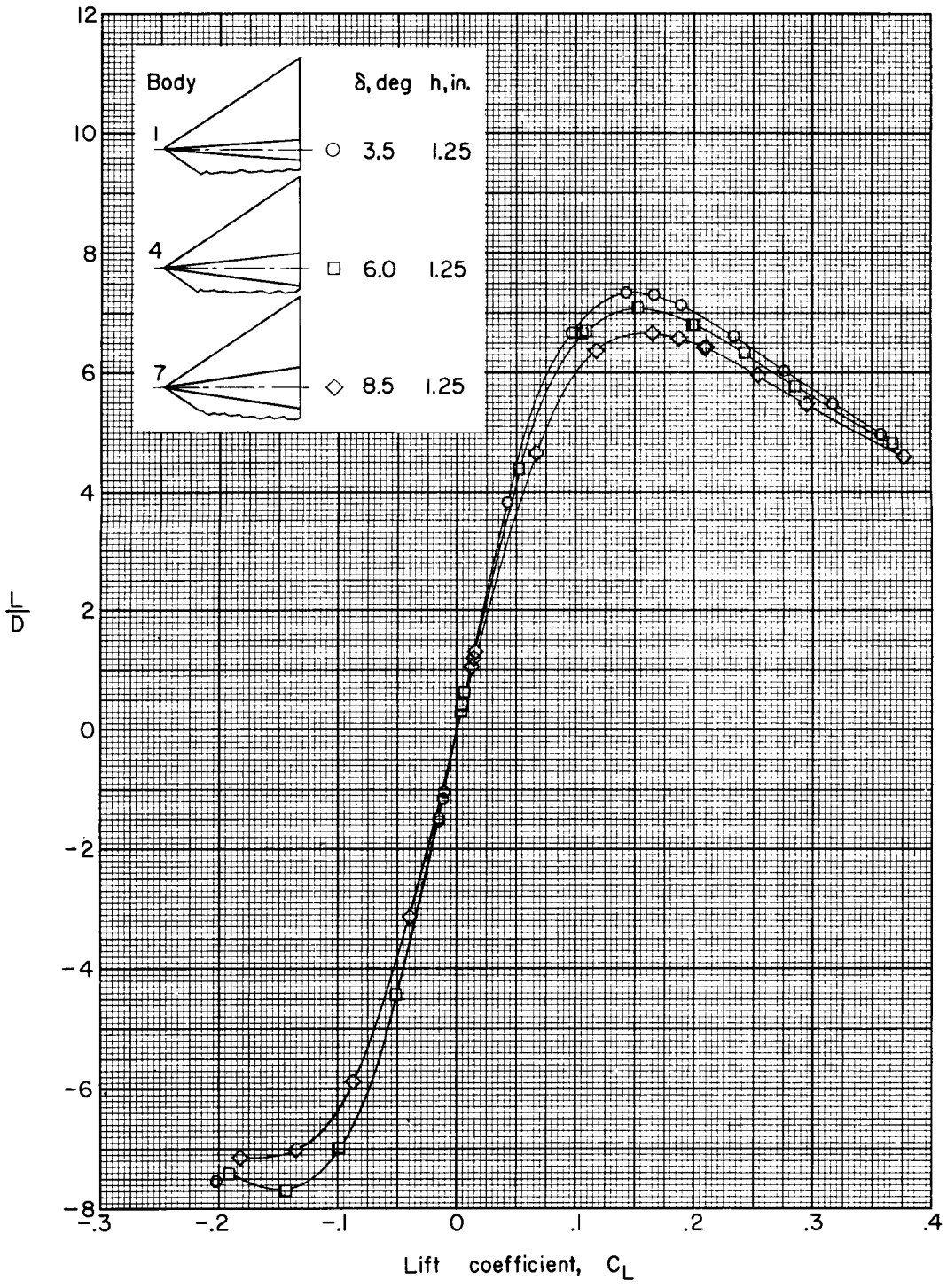

(b) Variation of L/D with C_L.

Figure 4.- Concluded.

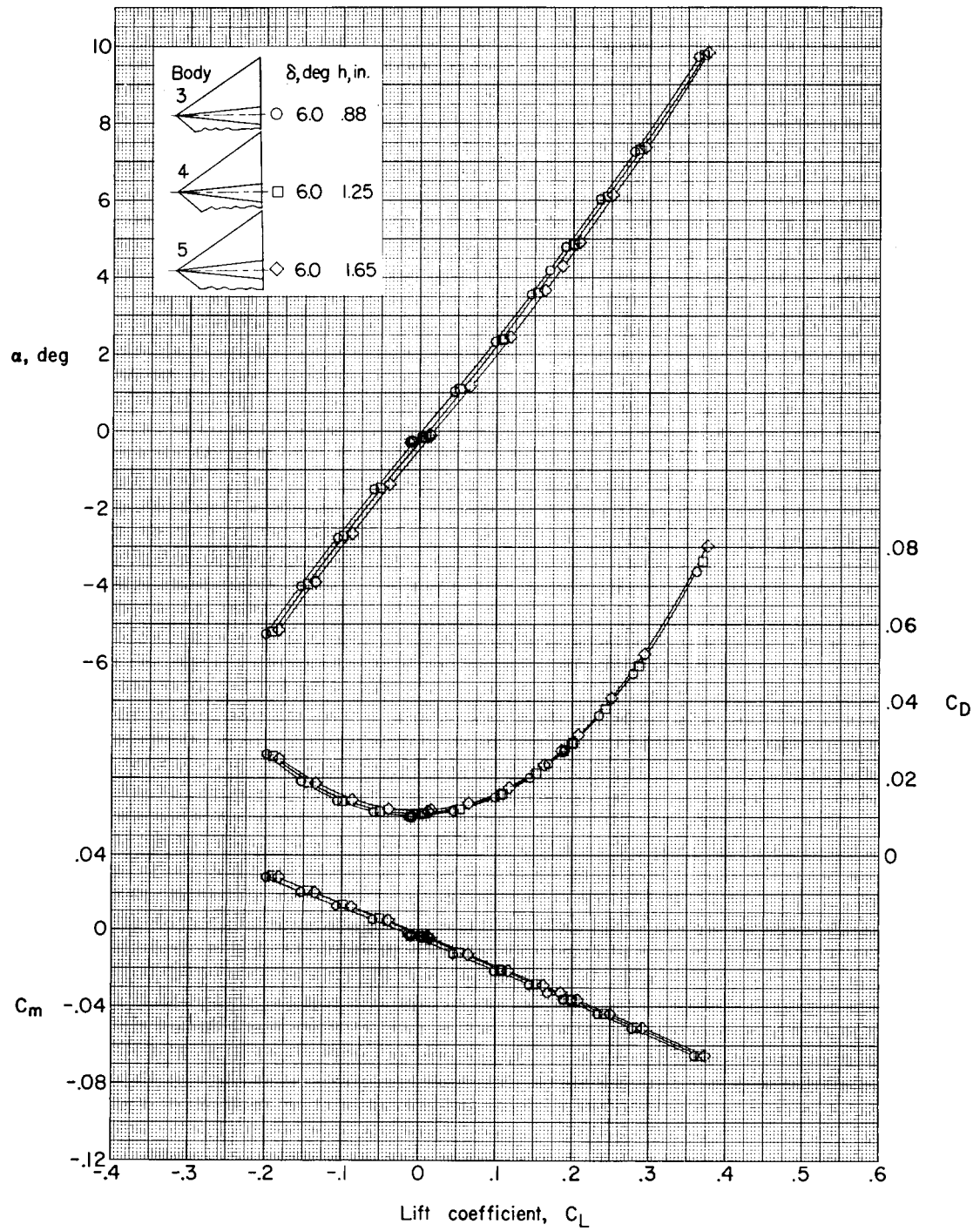

(a) Variation of α, C_m, and C_D with C_L.

Figure 5.- Effect of change in wedge vertical height on the aerodynamic characteristics of the wing-body combination. Body A located above wing.

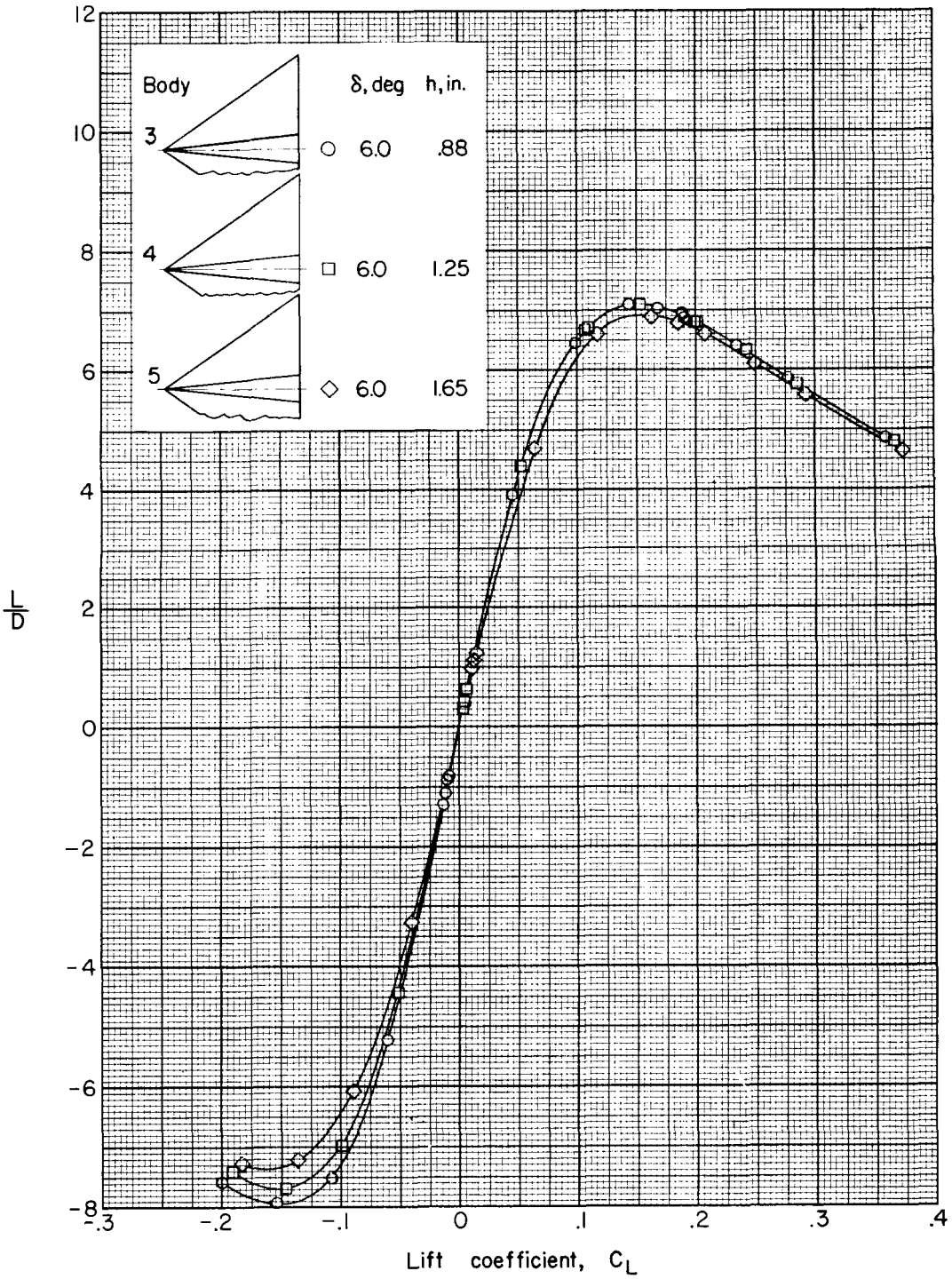

(b) Variation of L/D with C_L.

Figure 5.- Concluded.

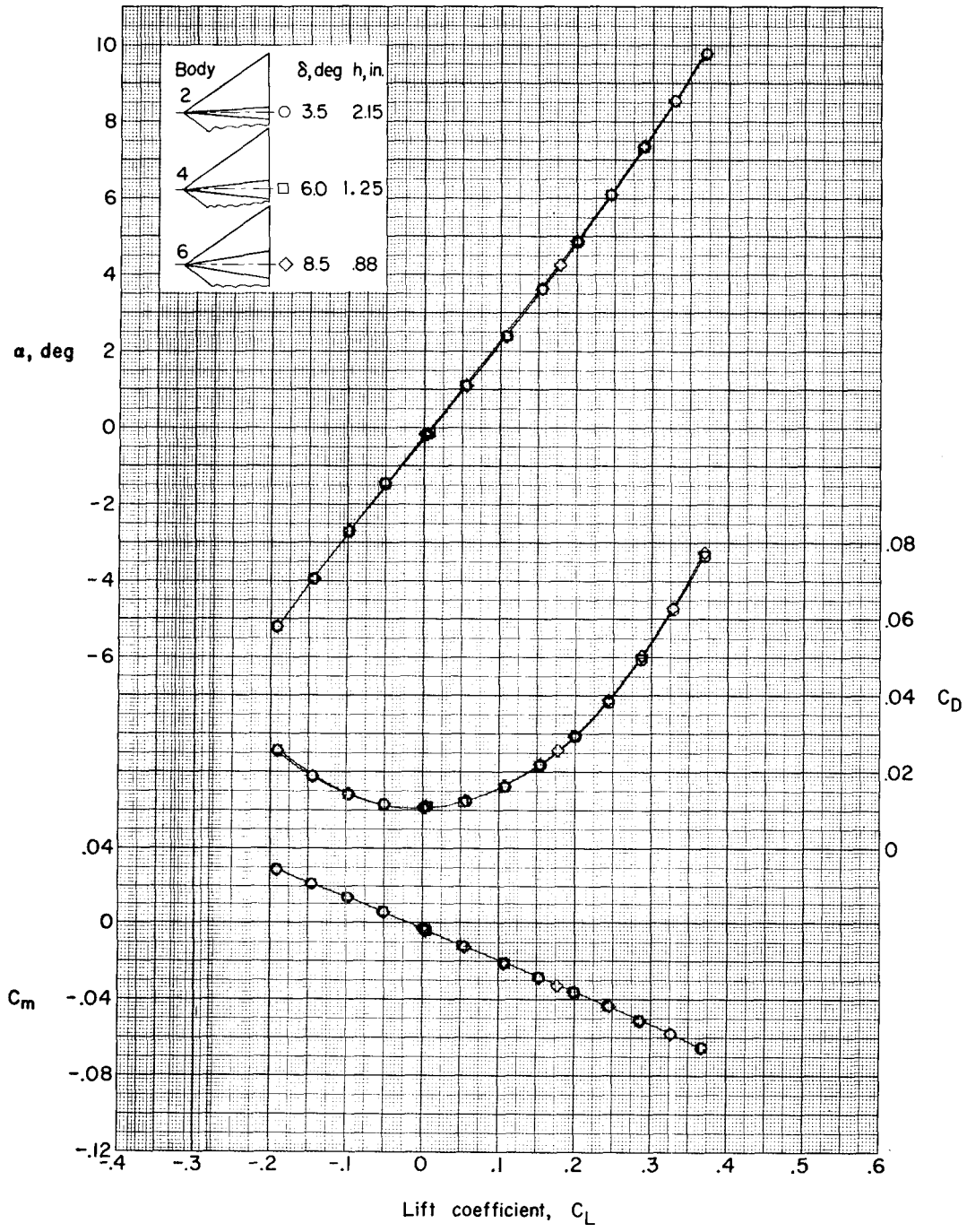

(a) Variation of α, C_m, and C_D with C_L.

Figure 6.- Effect of change in body shape at constant volume $\left(\frac{V^{2/3}}{S} = 0.057\right)$ on aerodynamic characteristics of wing-body combination. Body A located above wing.

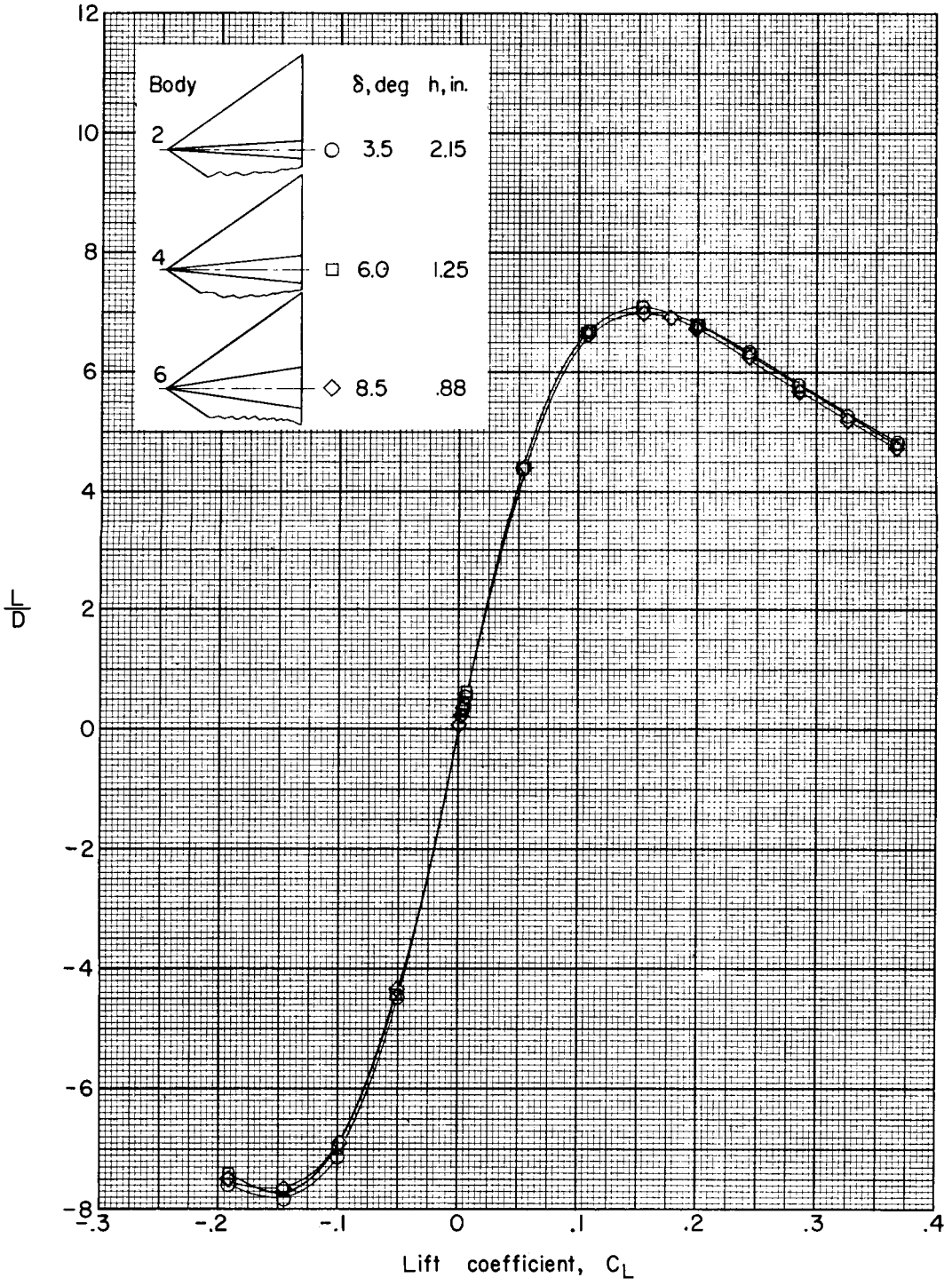

(b) Variation of L/D with C_L.

Figure 6.- Concluded.

body having a shallow afterbody wedge beginning at the wing leading edge and extending to the wing trailing edge. The data for this wing-body combination are similar to those of the three preceding configurations in figure 7.

The results for the models with body A located below the wing (figs. 7 and 8, together with the basic data of fig. 3) indicate some other interesting wing-body interference effects. For example, the wing-body interference effects at zero angle of attack produce a positive lift increment so that the lift-drag polars are slightly displaced from zero lift in a manner similar to that for twisted and cambered wings. This effect results in a significant value of L/D even at zero angle of attack, and the maximum values of L/D are substantially greater for the positive lift range than for the negative lift range. In addition, the pitching-moment data for these models show that a favorable positive pitching moment is obtained which tends to shift the C_m trim point toward the C_L corresponding to maximum L/D.

The large changes in L/D values due to wing-body interference do not necessarily mean that similar changes would be expected for configurations with more conventional high fineness ratio bodies, since the minimum drag and the interference lift of a more streamlined body would probably be less than those for the present bodies. However, it does indicate that wing-body interference effects are potentially large, and care should be exercised in the design of airplane configuration in order to avoid wing-body shapes or component arrangements which might produce undesirable interference effects. A comparison of the maximum L/D values for any of the combined body configurations with the value for the basic wing-body configuration indicate that addition of the test bodies to the basic wing-body configuration always reduced the maximum L/D.

CONCLUDING REMARKS

An investigation has been conducted in the Langley 4- by 4-foot supersonic pressure tunnel at a Mach number of 2.01 in order to determine the interference effects produced by several wedge-shaped bodies located above and below a delta-wing configuration. The results indicate that large changes in the maximum lift-drag ratios due to wing-body interference effects were obtained for the combined wedge-shaped bodies located on both upper and lower surfaces of the wing. However, for all of the wedge-shaped bodies tested, addition of the bodies to the wing reduced the maximum lift-drag ratio from that of the basic wing-body combination. The interference effects of the two bodies in combination with the wing produced a favorable positive pitching-moment increment. For the range of body combinations tested, the magnitude of the lift-drag ratios is dependent to a great extent on the variation in body volume.

Langley Research Center,
National Aeronautics and Space Administration,
Langley Station, Hampton, Va., April 18, 1963.

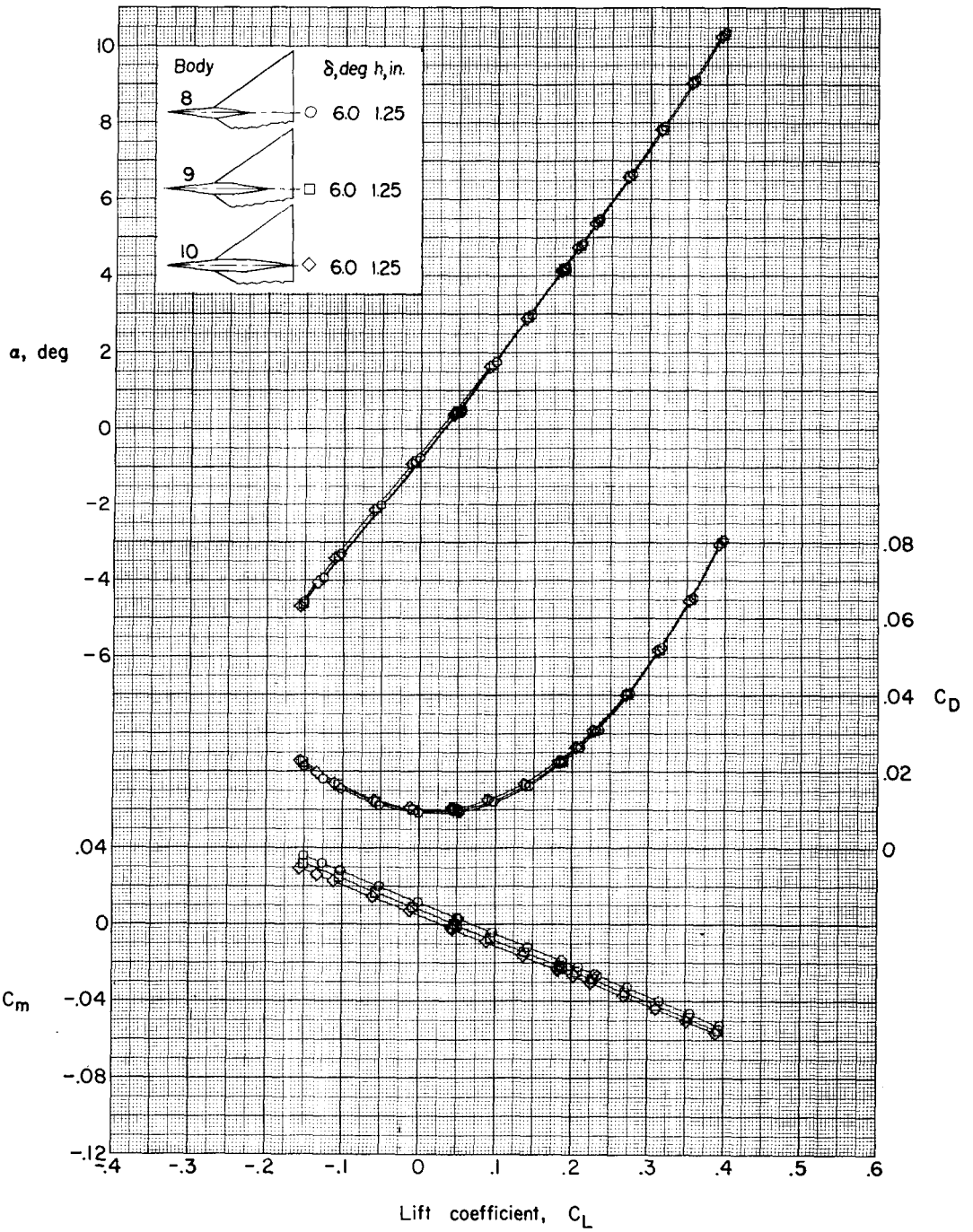

(a) Variation of α, C_m, and C_D with C_L.

Figure 7.- Aerodynamic characteristics of three wing-body combinations with wedge-shaped bodies having different body lengths. Body A located below wing.

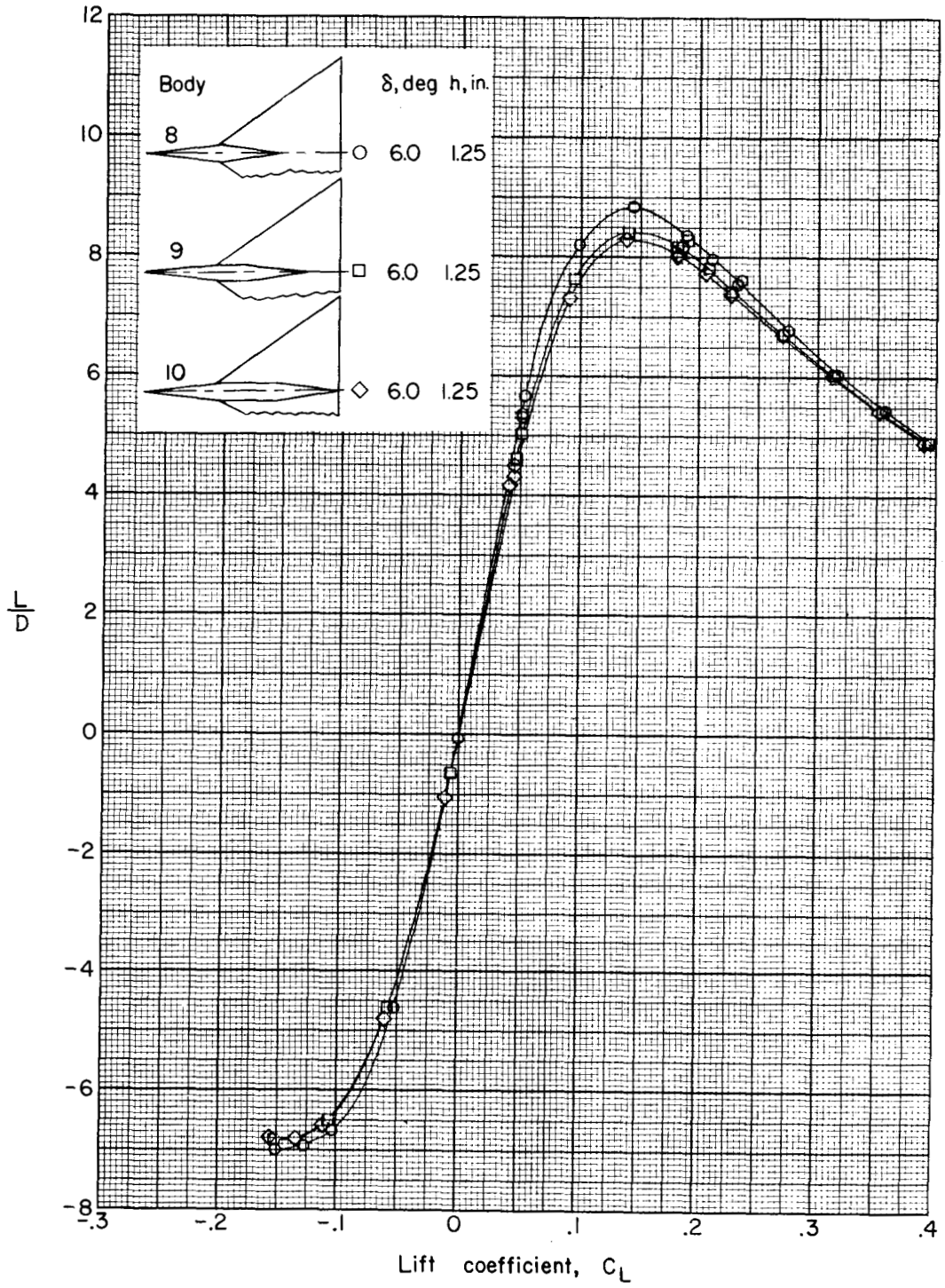

(b) Variation of L/D with C_L.

Figure 7.- Concluded.

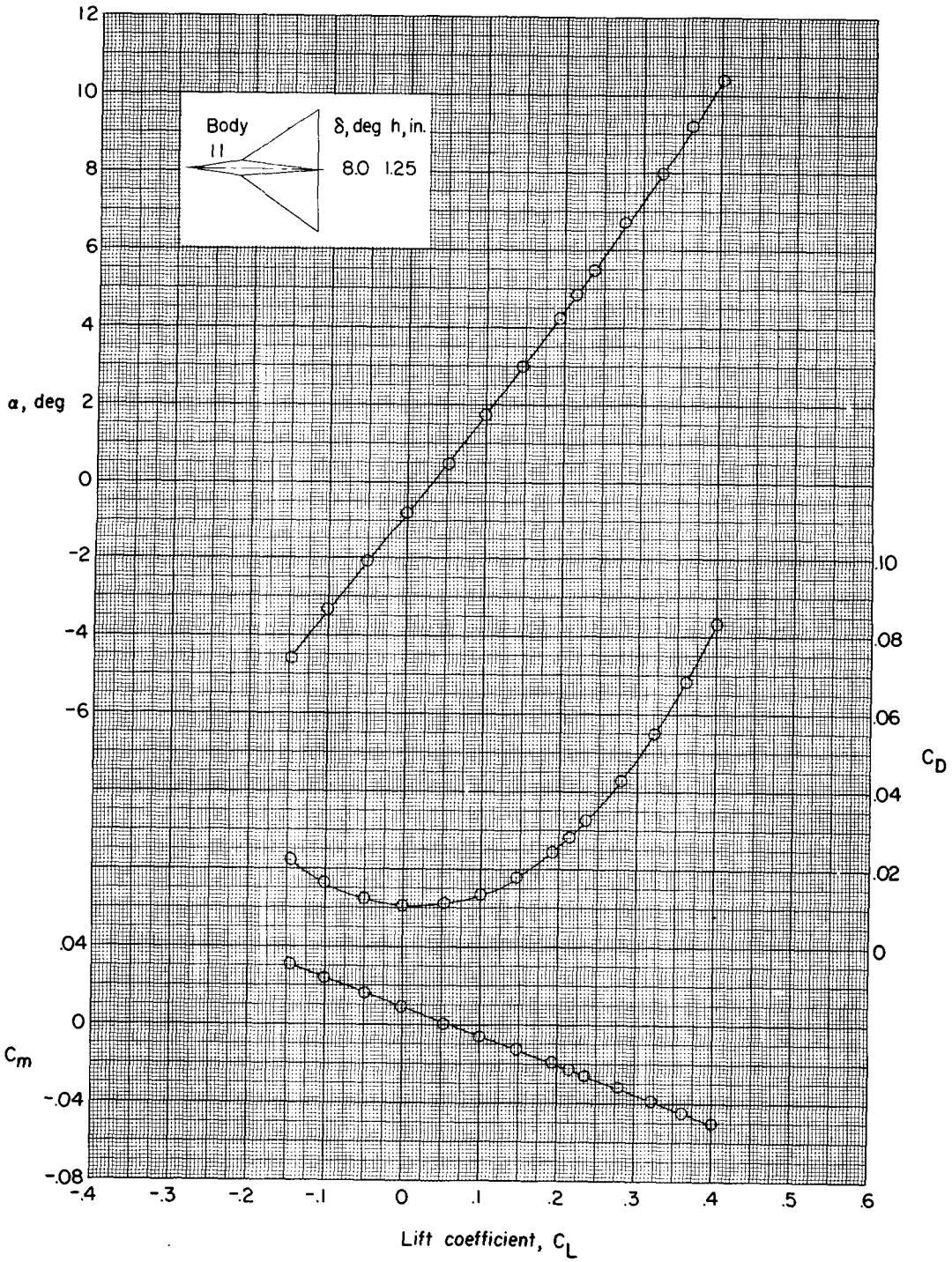

(a) Variation of α, C_m, and C_D with C_L.

Figure 8.- Aerodynamic characteristics of the wing-body combination with the large wedge-shaped body. Body A located below wing.

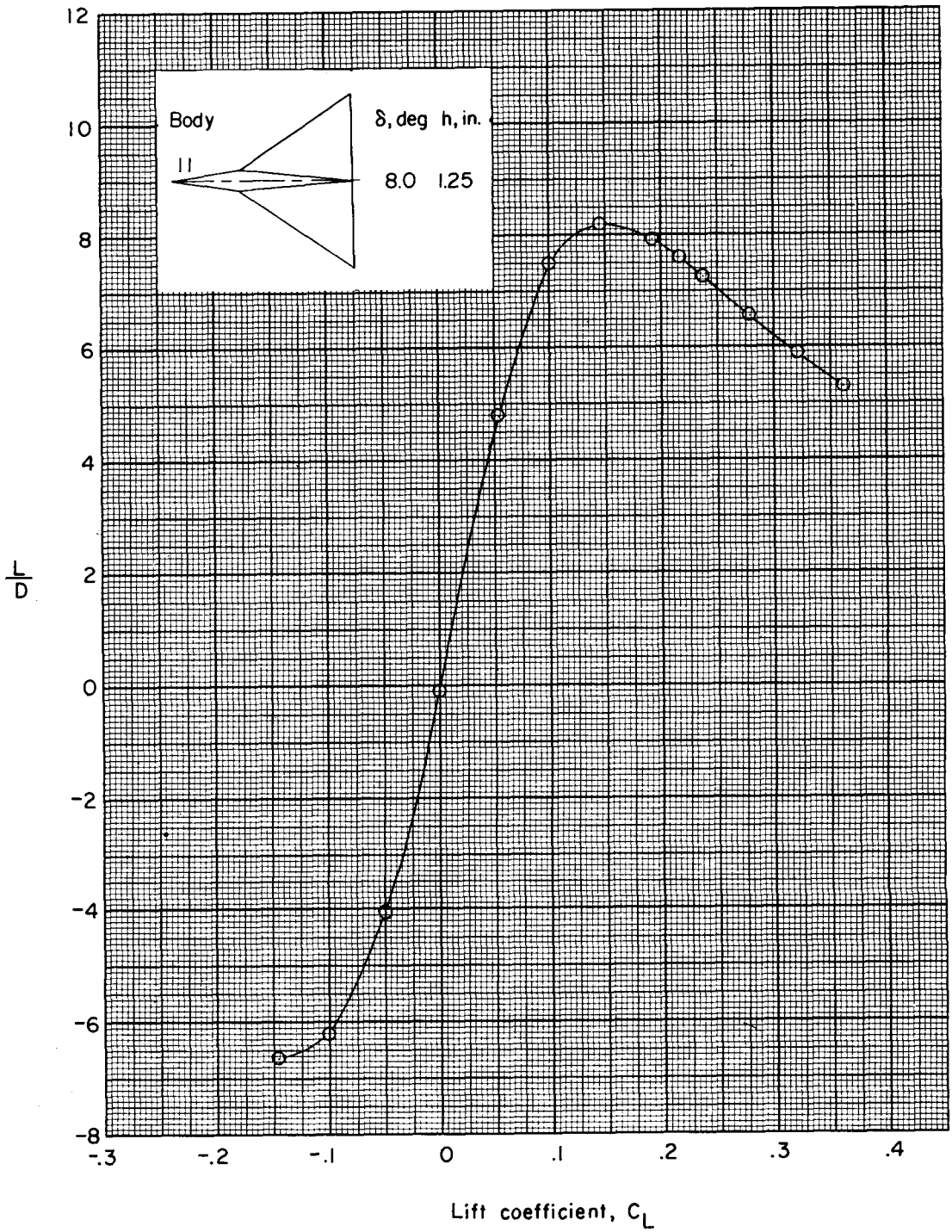

(b) Variation of L/D with C_L.

Figure 8.- Concluded.

REFERENCES

1. Ferri, Antonio, Clarke, Joseph H., and Casaccio, Anthony: Drag Reduction in Lifting Systems by Advantageous Use of Interference. PIBAL Rep. No. 272 (Contract No. AF 18(600)-694), Polytechnic Inst. Brooklyn, May 1955.

2. Rossow, Vernon J.: A Theoretical Study of the Lifting Efficiency at Supersonic Speeds of Wings Utilizing Indirect Lift Induced by Vertical Surfaces. NACA RM A55L08, 1956.

3. Eggers, A. J., Jr., and Syvertson, Clarence A.: Aircraft Configurations Developing High Lift-Drag Ratios at High Supersonic Speeds. NACA RM A55L05, 1956.

4. Hasel, Lowell E.: An Experimental Pressure-Distribution Investigation of the Interference Effects Produced at a Mach Number of 3.11 by Wedge-Shaped Bodies Located Under a Triangular Wing. NASA TM X-76, 1959.

NASA-Langley, 1963 L-3390